LPA_1 is essential for lymphatic vessel development in zebrafish

Shyh-Jye Lee,[*,†,1] Tun-Hao Chan,[*,2] Tzu-Cheng Chen,[*,2] Bo-Kai Liao,[‡] Pung-Pung Hwang,[‡] and Hsinyu Lee[*,†,1]

*Institute of Zoology and †Department of Life Science, National Taiwan University, Taipei, Taiwan; and ‡Institute of Cellular and Organismic Biology, Academia Sinica, Taipei, Taiwan

ABSTRACT **Lysophosphatidic acid (LPA) has long been implicated in regulating vascular development *via* endothelial cell-expressed G protein-coupled receptors. However, because of a lack of notable vascular defects reported in LPA receptor knockout mouse studies, the regulation of vasculature by LPA receptors *in vivo* is still uncertain. Using zebrafish as a model, we studied the gene expression patterns and functions of an LPA receptor, LPA_1, during embryonic development, in particular, vascular formation. Whole-mount *in situ* hybridization experiments revealed that zebrafish lpa_1 ($zlpa_1$) was ubiquitously expressed early in development, and its expression domains were later localized to the head region and the vicinity of the dorsal aorta. The expression of $zlpa_1$ surrounding the dorsal aorta suggests its role in vasculature development. Knocking down of $zLPA_1$ by injecting morpholino (MO) oligonucleotides at 0.625–1.25 ng per embryo resulted in the absence of thoracic duct and edema in pericardial sac and trunk in a dose-dependent manner. These $zlpa_1$-MO-resulted defects could be specifically rescued by ectopic expression of $zlpa_1$. In addition, overexpression of *vegf-c*, a well-known lymphangiogenic factor, also partially ameliorated the inhibition of thoracic duct development. Taken together, these results demonstrate that LPA_1 is necessary for lymphatic vessel formation during embryonic development in zebrafish.—Lee, S.-J., Chan, T.-H., Chen, T.-C., Liao, B.-O., Hwang, P.-P., Lee, H. LPA_1 is essential for lymphatic vessel development in zebrafish. *FASEB J.* 22, 3706–3715 (2008)**

Key Words: lysophosphatidic acid · G protein-coupled receptor · endothelial cell · thoracic duct · morpholino

A COMPLEX VASCULATURE NETWORK exists for the adequate exchange of gases, nutrients, signal molecules, and cells circulating between tissues and organs in vertebrates. This highly branched vasculature is mainly composed of blood and lymphatic vascular systems. Both types of vessels are assembled by a lining of endothelial cells (ECs). Vasculogenesis begins in the early gastrulation stage when primary axial vessels are formed, followed by angiogenesis for branching into the entire blood-conveyance network (1). After formation of the blood network, the lymphatic system develops blind-ended capillaries, which converge into a larger collecting duct (the thoracic duct), ultimately merging into the anterior venous (2). The formation of the entire vasculature network depends on the precise molecular control of proliferation, migration, and assembly of ECs, and also EC signaling for destabilizing and stabilizing the vasculature (1). Understanding endothelial signaling during development in both embryonic and adult tissues is crucial in providing insights into the regulation of development and certain disease conditions such as cancer (3).

Lysophosphatidic acid (LPA), a bioactive lipid, has diverse cellular (4) and signaling functions *via* its cognate cell surface G protein-coupled receptors (5, 6), and it has been implicated as having an emerging role in a variety of cancers (4). LPA receptor 1 (LPA_1) of the endothelial differentiation gene (Edg) subfamily (7) was the first receptor identified for LPA (8). The lpa_1 gene is ubiquitously expressed at high levels in the colon, small intestine, placenta, brain, and heart, and moderately expressed in the pancreas, ovaries, and prostate (8). Because of its high enrichment in the neurogenic ventricular zone, the lpa_1 gene was previously called *ventricular zone gene-1* (*vzg-1*), and research mainly focused on studying its role in brain neurogenesis. A knockout mouse study initially failed to identify a role for LPA_1 in the developing brain (9). However, a study using a variant of LPA_1-null mice propagated from the original LPA_1 knockout mice, the so-called $maLPA_1$ mice, did exhibit a reduced ventricular zone, altered neuronal markers, and increased cell death (10). Recently, we have demonstrated that LPA_1 is highly expressed in human umbilical vascular endothelial cells (HUVECs) (11). The high expression of LPA_1 in ECs is very intriguing, as LPA has been suggested to play an important role in angiogenesis (12). In addition, the LPA_1 was demonstrated to link pulmonary fibrosis to lung injury by regulating fibroblast recruit-

[1] Correspondence: 1 Roosevelt Rd., Section 4, Institute of Zoology, National Taiwan University, Taipei, Taiwan 106, R.O.C. E-mail: S.-J.L., jefflee@ntu.edu.tw; H.L., hsinyulee@ntu.edu.tw

[2] These authors contributed equally to this work.

doi: 10.1096/fj.08-106088

0892-6638/08/0022-3706 © FASEB

ment and vascular leak (13). LPA can regulate human EC proliferation (14, 15), migration (14, 15), capillary-like tube formation *in vitro* (16), activation of proteases (17), expression of inflammation-related genes (18), and endothelial permeability (19). It also mediates contractility, proliferation, and differentiation of vascular smooth muscle cells (20–24). Unsaturated LPA has been shown to trigger rat blood vessel remodeling *in vivo* (25). Moreover, knocking out a synthesizing enzyme of LPA, autotaxin, causes lethality in mice on embryonic day 9.5, with profound vascular defects in the yolk sac (26). These results suggest that LPA is essential for blood vessel formation during development. However, none of the LPA receptor knockout studies, including those using LPA_1 (9), LPA_2 (27), and LPA_3 (28) null-mice, reported defects in the vasculature except for a low incidence of cranial hemorrhage in LPA_1 and LPA_1/LPA_2 null mice (9, 27). Whether other recently identified LPA receptors, such as LPA_4 (29) and LPA_5 (30), or complementary effects between LPA receptors, might have caused the lack of detectable vascular defects in those LPA receptor knockout mice is unclear. Thus, the role of LPA receptors in vascular development has remained an unresolved issue.

To study LPA receptor function, especially its role in vascular formation, we identified an *lpa$_1$* gene in zebrafish, which is a well-established model for angiogenesis research (31, 32). We demonstrate that knocking down LPA_1 translation results in inhibition of thoracic duct formation. In addition, these defects could be fully rescued by the ectopic expression of *lpa$_1$* and partially ameliorated by a lymphangiogenic factor, *vegf-c*. Taken together, these results suggest that LPA_1 functions as a critical regulator directing lymphatic vessel development.

MATERIALS AND METHODS

Maintenance of zebrafish

Breeding wild-type (AB) and transgenic zebrafish (*Tg(fli1:EGFP)^{y1}* from the Zebrafish Information Research Center (Eugene, OR, USA) were cultured at 27–28°C on a 14-h light/10-h dark cycle. Embryos were collected by natural spawning, raised in 0.3× Danieau's buffer [by diluting 1× Danieau's buffer: 58 mM NaCl, 0.7 mM KCl, 0.4 mM $MgSO_4$, 0.6 mM $Ca(NO_3)_2$, and 5.0 mM HEPES (pH 7.6), with double-distilled water] supplemented with 50 μg/ml streptomycin and 50 μg/ml penicillin G at 28.5°C until observation or fixation. Embryos were staged according to Kimmel *et al.* (33), and stages are given as hours or days postfertilization (hpf or dpf, respectively). All animal handling procedures followed the guidelines for the use of laboratory animals at National Taiwan University, Taipei, Taiwan.

Cloning and analysis of the zebrafish *lpa$_1$* gene

A reverse-transcription polymerase chain reaction (RT-PCR) was performed on total RNAs extracted from embryos at the designated times using the TRIzol reagent (Invitrogen, Carlsbad, CA, USA), according to the manufacturer's instructions. RNAs were subsequently treated with DNase I (Invitrogen), and first-strand complementary (c) DNAs were synthesized. cDNAs were generated from total RNAs of 24-hpf zebrafish larvae by reverse transcription using the M-MLV reverse transcription kit (Promega, Madison, WI, USA). A 1208-base pair (bp) DNA fragment containing the coding region of the zebrafish *lpa$_1$* gene (*zlpa$_1$*, *NM_001004502*) was amplified from zebrafish embryo cDNAs by PCR using primers with the following sequences: 5′-GCGAGTGATTTCTGGACCTTTCAGC-3′ (forward) and 5′-GCCTTTTTCACAGTCTCTTCTTGCG-3′ (reverse). The amplified PCR fragment was subcloned into a pGEM-T easy vector (Promega) for sequence verification. Amino acid sequences of LPA_1 from different species among chordates were identified from the National Center for Biotechnology Information (NCBI) database and aligned using the Vector NTI software (Invitrogen). The phylogenetic tree was constructed and drawn using the MEGA3 software (Biodesign Institute, Tempe, AZ, USA).

RT-PCR analysis

RNAs and cDNAs from embryos at designated stages and from different adult tissues were prepared as described previously. A 136-bp *zlpa$_1$* fragment was amplified with the following primers: 5′-CGGAGGGTAGTTGTGGTTATAG-3′ (forward) and 5′-GGTACGAGTTGCTGTAGAGTG-3′ (reverse). Amplification of a 542-bp *ef1α* fragment served as the RT-PCR internal control using the following primers: 5′-CAAGGAAGTCAGCGCATACA-3′ (forward) and 5′-TGATGACCTGAGCGTTGAAG-3′ (reverse).

Whole-mount *in situ* hybridization (WISH)

Embryos were grown to desired stages, fixed in 4% paraformaldehyde in phosphate-buffered saline (PBS) overnight, and manually dechorionated using fine forceps. Embryos were then stored in 100% methanol at −20°C until use. Antisense digoxigenin (DIG) -labeled RNA riboprobes were synthesized according to the manufacturer's instructions (Roche Applied Science, Penzberg, Germany). Hybridization and detection with an alkaline phosphatase-coupled anti-DIG antibody (Roche Applied Science) were performed according to Thisse *et al.* (34). Photographs were taken with a Nikon Coolpix995 digital camera (Nikon, Tokyo, Japan). The image background was adjusted to the white point by the Curves tool of Adobe Photoshop (Adobe Systems, San Jose, CA, USA), and all channel output levels were set to 228. For cryosections, stained samples were immersed in PBS containing 30% sucrose overnight, and embedded in optimal cutting temperature (OCT) compound embedding medium (Sakura, Tokyo, Japan) at −20°C, and 10-μm frozen cross-sections were cut with a CM 1900 rapid sectioning cryostat (Leica, Heidelberg, Germany) and attached to poly-L-lysine-coated slides (Electron Microscopy Sciences, Ft. Washington, PA, USA). Bright-field images were acquired with a TCS-SP5 confocal laser scanning microscope with a Leica HCX PL-APO ×63/1.30 glycerol objective (Leica Lasertechnik, Heidelberg, Germany) using a laser wavelength at 405 nm.

Morpholino oligonucleotides

Antisense morpholinos (MOs) were purchased from Open Biosystems (Huntsville, AL, USA) or custom made by Gene Tools (Philomath, OR, USA). To knockdown *zlpa$_1$* gene activity, we used two nonoverlapping MOs targeting the boundaries flanking exon 2 to interfere with its splicing. The first splice-blocking MO was designated sMO_1 (sequence:

5′-TGGAGCACTTACCCAATACAATCAC-3′), which targets the boundary between exon 2 and intron 2 (−13 to +12). The second splice-blocking MO was designated sMO_2 (sequence: 5′-GGTCTGTTTCTGAAAAGTAAAGATA-3′), which targets the boundary between intron 1 and exon 2 (−16 to +9). A 5-bp mismatched splice-blocking MO of sMO_1 was generated to serve as a control with the following sequence, with the mismatched pairs in lowercase letters: 5′-TGcAGgACTTACCgAATAgAATgAC-3′. In addition, a reported zebrafish *vegf-c* (*zvegf-c*) MO (35) (with the sequence: 5′-GAAAATCAAATAAGTGCATTTTAG-3′) was purchased from GeneTools. The MOs were dissolved in sterile double-distilled water to 1 mM, stored at −20°C, and further diluted to the desired working concentrations in 1× Danieau's buffer with 0.5% phenol red and kept at 4°C before being used.

Expression vector construction

The cDNAs of coding regions of *zlpa$_1$* were amplified by RT-PCR and TA-cloned into the pcDNA3.1/V5-His-TOPO vector designed to express proteins with V5 and 6-histidine double fusions at the C-terminal under the CMV promoter (Invitrogen). The primers used were as follows: 5′-ATTGCGGCCGCCATGGATGATAGACAATGCTA-3′ (*zlpa$_1$*, forward), 5′-ATTCTCGAGACCACTGAATGGTCATTATGGTGA-3′ (*zlpa$_1$*, reverse). The z*vegf-c* in the same expression vector as *zlpa$_1$* was kindly provided by C. C. Huang (Institute of Cellular and Organismic Biology, Academia Sinica, Taipei, Taiwan).

Microinjection procedures

Microinjections were carried out according to Lai *et al.* (36). Briefly, embryos at desired stages were immobilized in an injection trough on a 90-mm 2% agar plate. MOs or expression vectors were prepared as described at designated concentrations. An injection volume from 0.5–2.3 nl of different MOs, vectors, or vehicles was injected into 1-cell-stage embryos. After injection, embryos were recovered from the injection troughs and cultured in 0.3× Danieau's buffer until being examined.

Photographs of vascular and lymphatic vessels

Blood or lymphatic vessels of *Tg(fli1:EGFP)^{y1}* zebrafish were observed under a DM5000B epifluorescent microscope (Leica, Wetzlar, Germany) with Leica HC PL Fluotar objectives using a fluorescein isothiocyanate (FITC) or rhodamine filter cube and imaged using a $CoolSNAP_{fx}$ CCD camera (Roper Scientific, Tucson, AZ, USA). The images were acquired using the SimplePCI program (ver. 5.2; Compix, Cranberry Township, PA, USA) and pseudocolored using green or red color for the FITC or rhodamine images, respectively.

Statistical analysis

All experimental values are presented as mean ± SD and were analyzed by paired-sample Student's *t* test in Microsoft Excel (Microsoft, Redmond, WA, USA).

RESULTS

Cloning, sequencing, and expression profile analysis of *lpa$_1$*

To investigate the roles of LPA_1 during embryonic development, we first identified an *lpa$_1$* gene (*NM_001004502*) from the NCBI database and isolated a 1208-bp DNA fragment by PCR amplification from zebrafish embryo cDNAs. This DNA fragment was subcloned, sequenced, and found to be 100% matched to the reported *lpa$_1$* sequence from 141 to 1348 nucleotides of *NM_001004502*. It is referred as *zlpa$_1$* hereafter. The gene, *zlpa$_1$*, encodes a protein with 346 amino acids and a predicted molecular weight of 39.6 kDa. We aligned the translated amino acid sequences of zebrafish, mouse (*NP_034466*), and human (*NP_001392*) LPA_1, and we found that they were highly homologous with a sequence identity of 85% (**Fig. 1*A***). A phylogenic analysis showed that zebrafish LPA_1 is most closely related to the LPA_1 of Fugu (*Takifugu rubripes*) among chordates (Fig. 1*B*). To understand the chromosomal location of *lpa$_1$*, we performed a syntenic analysis of these *lpa$_1$* genes. The *lpa$_1$* gene is located at chromosomes 10, 4, and 9 in the zebrafish, mouse, and human, respectively. They all have the same orientation and are positioned next to *musk*, a muscle-specific kinase receptor gene (Fig. 1*C*). Collectively, these results suggest that z*lpa$_1$* is evolutionarily related to mammalian *lpa$_1$* genes.

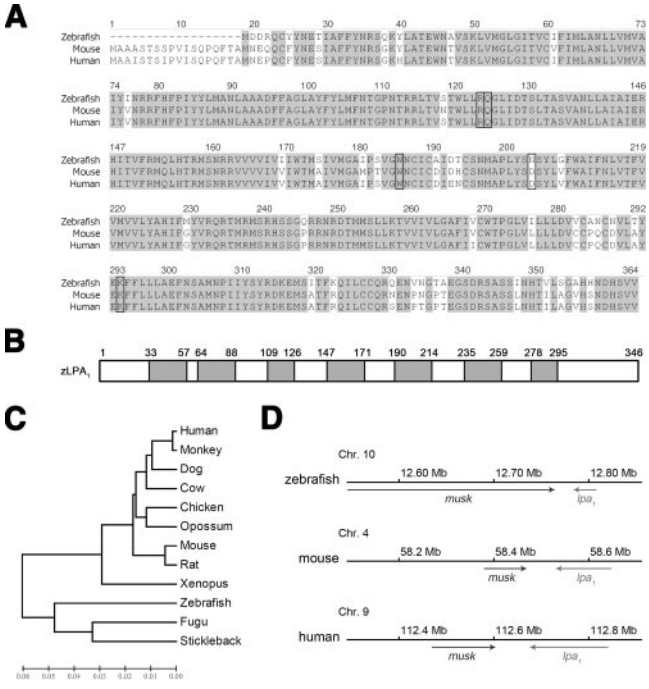

Figure 1. Sequence analysis of the zebrafish LPA receptor, $zLPA_1$. *A*) Amino acid sequence alignment of $zLPA_1$ with its human and mouse homologs. Identical amino acids are shaded in gray. The putative LPA binding sites are enclosed by rectangles. *B*) The $zLPA_1$ amino acid sequence was analyzed by the HMMTOP 2.0 (http://www.enzim.hu/hmmtop/index.html). Seven predicted transmembrane domains are shown in gray boxes flanking boundary amino acid numberings. *C*) The phylogenic tree of LPA_1 homologs in chordates. The horizontal length is proportional to the estimated time from divergence of the gene from the related family member. *D*) Chromosomal location of the zebrafish, mouse and human *lpa$_1$* genes. The *lpa$_1$* gene is located at chromosome (Chr.) 10, 4, and 9 in the zebrafish, mouse, and human, respectively. They are all in the same orientation (left arrows) and located next to a muscle-specific kinase receptor gene, *musk* (right arrows).

To investigate the spatial and temporal expression patterns of $zlpa_1$, we synthesized its antisense riboprobe and used it for the WISH analysis. The WISH analysis revealed that $zlpa_1$ mRNAs were initially slightly expressed in the entire embryo before the completion of gastrulation. During somitogenesis, the $zlpa_1$ expression domain was restricted to adaxial cells flanking the notochord, head, and tail buds (**Fig. 2*A*, *B***). It was notable that 18-somite-stage embryos exhibited more-distinct individual $zlpa_1$ expression domains restricted to adaxial cells and adjacent somites compared to 6-somite-stage embryos. At 24 hpf, $zlpa_1$ was highly expressed in the anterior head region (including eyes, midbrain/hindbrain boundary, and brain mesoderm) and tail terminal. In addition, $zlpa_1$ expression was also observed in the dorsal aorta and vicinity (Fig. 2*C*). At the 31-hpf stage, the $zlpa_1$ expression domain was less prominent in the eyes and tail terminal but evident in brain mesoderm. In contrast, $zlpa_1$ expression still remained in the dorsal aorta and vicinity (Fig. 2*D*). Transverse sections of the trunk region of 31-hpf embryos showed that $zlpa_1$ was expressed in a portion of the dorsal aorta and vicinity, including hypochord. It was also sporadically observed in the outside peripheral muscle regions but was excluded from neural tube and notochord (Fig. 2*E*). Furthermore, to understand the $zlpa_1$ developmental gene expression profile, we analyzed its mRNA expression in zebrafish embryos at different stages from 1-cell to 7-dpf by RT-PCR. RT-PCR analysis showed that $zlpa_1$ was expressed in all early embryos and larvae up to 7 dpf (Fig. 2*F*) and in all adult tissues examined (Fig. 2*G*). The $zlpa_1$ was expressed at higher levels in the brain, eyes, ovaries, testes, gills, and swim bladder (Fig. 2*G*).

Antisense MO interferes with $zlpa_1$ splicing and results in pericardial and truck edema

To study the roles of $zLPA_1$ during early embryogenesis, we used antisense MO oligonucleotides to knockdown $zlpa_1$ gene activity. The $zlpa_1$ gene consists of 3 exons and 2 introns, and a translation start site (ATG) is located at the 5′ terminal of exon 2 (**Fig. 3*A***). Thus, we generated a splice-blocking MO (sMO_1), targeting the boundary between exon 2 and intron 2 to interfere with the splicing of exon 2. The sMO_1 was assumed to skip the transcription of exon 2, which subsequently would result in aberrant protein synthesis (Fig. 3*B*). By the RT-PCR analysis, we demonstrated that the sMO_1 caused a shortening of $zlpa_1$ transcripts from 1208 bp in untreated control embryos to 453 bp in sMO_1-treated embryos injected with 2.5 and 5 ng per embryo (Fig. 3*C*). The 453-bp PCR fragment was sequenced and compared to the 1208-bp fragment. Sequence comparison revealed that the exon 2 was not transcribed as expected (Supplemental Fig. S1). The similar effect was also observed in embryos treated with 1.25 ng per embryo. In addition, the $zlpa_1$-splice-blocking activity of sMO_1 remained active in treated embryos from 1 dpf to 5 dpf (Fig. 3*D*). Thus, we used $zlpa_1$-sMO_1 to explore LPA_1's function in zebrafish development.

To test the dosage response, we first injected different amounts (1.25–5 ng per embryo) of $zlpa_1$-sMO_1 into 1-cell stage embryos. The $zlpa_1$-sMO_1-treated embryos ($zlpa_1$ morphants) showed normal morphology during early development, but these $zlpa_1$ morphants gradually developed edema in the pericardial sac and body cavity (**Fig. 4*B***) compared to the normal appearance of untreated zebrafish larvae (Fig. 4*A*) after 4 dpf. Dose-

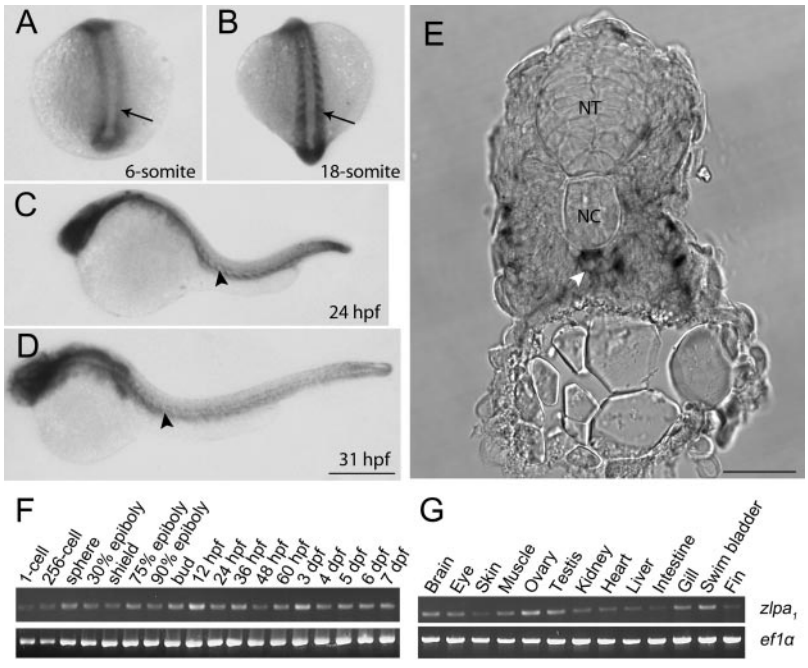

Figure 2. Expression patterns of $zlpa_1$. WISH was performed in embryos at designated stages using a $zlpa_1$ antisense riboprobe. Anterior is to the top (*A*, *B*) or left (*C*, *D*); dorsal and lateral views, respectively. A transverse section through the trunk (dorsal at the top) at the yolk extension region is also presented (*E*) *A*) Six-somite stage. The gene, $zlpa_1$, is expressed by adaxial cells (arrow), head, and tail bud. *B*) Eighteen-somite stage. The $zlpa_1$ expression domain still encompasses adaxial cells (arrow), head, and tail buds. More distinct individual $zlpa_1$ expression domains are shown in adaxial cells and vicinity. *C)* Twenty-four-hpf stage. The $zlpa_1$ gene is highly expressed in the anterior head region and tail terminal. In addition, $zlpa_1$ is expressed in the dorsal aorta (arrowhead) and vicinity. *D*) Thirty-one-hpf stage. The $zlpa_1$ expression domain is localized to the brain region and diminished in the eye and tail terminal. The $zlpa_1$ expression domain is still evident in the dorsal aorta (arrowhead) and vicinity. *E*) Thirty-one-hpf stage. A transverse section reveals that $zlpa_1$ RNAs are condensed in part of the dorsal aorta (white arrowhead). *F*, *G*) Expression of $zlpa_1$ was also examined by amplifying a 136-bp lpa_1 fragment (top gels) at different embryonic stages (*F*) and in adult tissues (*G*) by RT-PCR. A 524-bp *ef1*α fragment was also amplified to serve as an internal control (bottom gels). Scale bars = 1 mm (*A–D*); 20 μm (*E*).

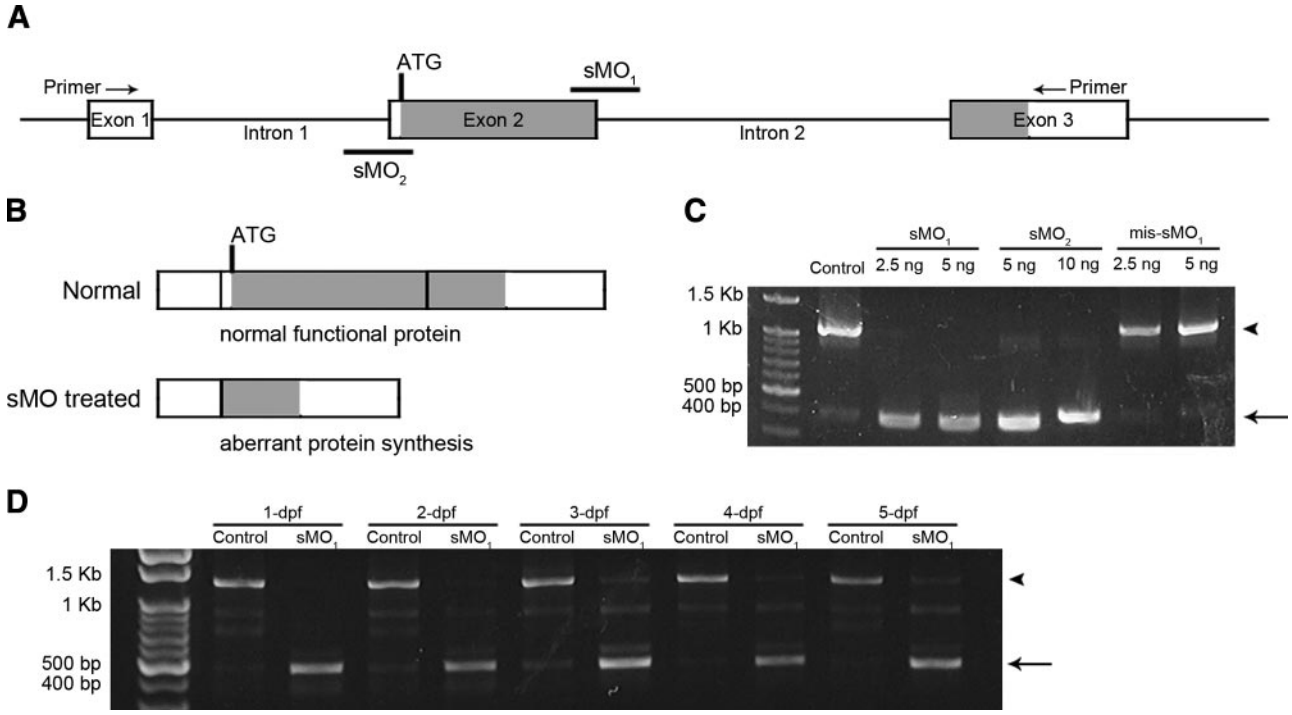

Figure 3. Antisense MOs induce splicing aberrant of *zlpa*$_1$. *A*) Diagram of a partial map of *zlpa*$_1$ genomic DNA. Exons and introns are shown in boxes and lines, respectively, and labeled with the corresponding exon or intron number. Two nonoverlapping *zlpa*$_1$ sMOs, sMO$_1$ and sMO$_2$, were designed to target the boundaries of exon 2/intron 2 and exon 2/intron 1, respectively. *B*) The sMOs presumably eliminated the transcription of exon 2, which contains the translation start site, and resulted in aberrant protein synthesis. *C*) RT-PCR analysis using a primer pair as indicated in *A* shows that both sMO$_1$ and sMO$_2$ caused the deletion of exon 2 and resulted in 453-bp PCR fragments (arrow) compared to the intact 1208-bp fragments (arrowhead) in control untreated and 5-bp mismatched sMO$_1$ (mis-MO$_1$) embryos. *D*) The *zlpa*$_1$ transcripts of 1- to 5-dpf embryos treated without (control) and with 1.25 ng sMO$_1$ per embryo was analyzed by RT-PCR as described.

dependently, these morphants also gradually showed blood flow retardation and failure in ventricle contraction (data not shown). Zebrafish embryos injected with 2.5 or 5 ng *zlpa*$_1$-sMO$_1$ appeared very unhealthy; therefore, to avoid possible complications generated by high dosages, we subsequently used 1.25 ng unless otherwise stated. This dosage resulted in milder cardiovascular defects in ~30% of treated embryos, while the rest of embryos appeared healthy.

zlpa$_1$ morphants exhibit defects in thoracic duct formation

At 1.25 ng *zlpa*$_1$-sMO$_1$, 41.4 ± 5.6% (n=78), embryos developed edema in the pericardial and trunk regions (Fig. 4*B*). This *zlpa*$_1$-sMO$_1$-induced edema differs from those frequently observed edemas in various drug-treated or mutant zebrafish that mainly occur in the pericardial region. Thus, we decided to further examine this aspect. The occurrence of edema indicates an accumulation of interstitial fluids, which might result from vascular leakage or a failure of lymphatic vessels to absorb fluids. To examine the integrity of the vasculature, we examined the effects of *zlpa*$_1$-sMO$_1$ in embryo vasculature using both wild-type and vasculature-fluorescent *Tg*(*fli1:EGFP*)^{y1} zebrafish (37). No obvious defects in vasculature were observed in morphants, except some distortions of the patterning of the dorsal longitudinal anastomic vessel (DLAV), intersegmenal vessels (ISVs), supraintestinal artery (SIA), and subintetinal vein (SIV) after 5 dpf that might be caused by edema (data not shown).

To observe the lymphatic vasculature, we adapted an approach developed by two independent laboratories (38, 39) to monitor the development of lymphatic vessels in the presence or absence of *zlpa*$_1$-sMO$_1$. We successfully recorded the development of the thoracic duct, the largest lymphatic vessel connecting to the cardinal vein, in a zebrafish larva from 3 to 5 dpf (see Supplemental Fig. S2). The thoracic duct initially forms

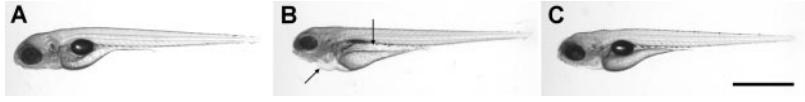

Figure 4. Ectopic expression of *zlpa*$_1$ rescues the splice-blocking MO induced edema. Zebrafish embryos were untreated (*A*) or injected with 1.25 ng *zlpa*$_1$ sMO$_1$ (*B, C*). Edema appeared in the pericardial sac and gut vicinity (arrows) in 5-dpf morphants (*B*). The *zlpa*$_1$ sMO$_1$-induced edema was notably reduced by coinjecting 100 pg of the pcDNA 3.1 vector with *zlpa*$_1$ (*C*). Scale bar = 1 mm.

as isolated islands (Supplemental Fig. S2*A*, *B*), and the fusing of these islands gives rise to a complete vessel with lumen (Supplemental Fig. S2*C*, *D*). These observations were similar to those reported by Yaniv *et al.* (39). In 5-dpf *zlpa*$_1$ morphants, thoracic ducts did not form (**Fig. 5*B*, *F***) compared to those control ones with normal thoracic ducts (Fig. 5*A*, *C*). Although only some of the *zlpa*$_1$ morphants injected with 1.25 ng *zlpa*$_1$-sMO$_1$ exhibited mild cardiovascular defects, it was still possible that the absence of thoracic ducts in those *zlpa*$_1$ morphants might be a nonspecific secondary effect of cardiovascular defects. To further clarify this issue, we injected *Tg*(*fli1:EGFP*)^{y1} zebrafish embryos with 0.625 ng sMO$_1$. We found no notable cardiovascular defects in the treated embryos, and examined the integrity of their thoracic ducts. In four trials, 87.1 ± 17.7% of 46 *zlpa*$_1$ morphants showed defects in thoracic duct formation. Although the penetrance was lower and less consistent at this dosage, the experiment did show that the inhibition of thoracic duct formation by *zlpa*$_1$-sMO$_1$ was specific and not secondary to the cardiovascular defects. In addition, we also tested the function of the thoracic duct using an intramuscular injection of rhodamine dextran and observed that the injected rhodamine dextran was absorbed by the thoracic duct of the untreated zebrafish (Fig. 5*D*, *E*), but not that of the *zlpa*$_1$ morphants (Fig. 5*G*, *H*).

To assure the specificity of *zlpa*$_1$-sMO$_1$ in inhibiting thoracic duct formation and induction of edema, we examined the effects on zebrafish development of an sMO$_1$ 5-bp mismatched MO (mis-sMO$_1$) and another *zlpa*$_1$ splice-blocking MO, sMO$_2$, which targets the boundary between intron 1 and exon 2. RT-PCR analysis showed that the mis-sMO$_1$ had no effect on *zlpa*$_1$ transcript formation at up to 5 ng per embryo. In contrast, the sMO$_2$ caused missplicing of exon 2, as did sMO$_1$, but some residual transcripts still remained intact, even when a higher amount of MO (10 ng/embryo) was used (Fig. 3*C*). Sequence analysis of *zlpa*$_1$ transcripts in those mis-sMO$_1$ and sMO$_2$ morphants demonstrated that they had the same sequences as those of control and sMO$_1$-treated embryos, respectively (Supplemental Fig. S1). Using the numbers of segments between ISVs encompassed by the thoracic duct as an index, we analyzed the effects of different *zlpa*$_1$ MOs on the formation of the thoracic duct. We considered a thoracic duct with >6 segments in length in the examined region as normal. In three independent experiments, 100.0 ± 0.0% of both the control and the mis-sMO$_1$-treated embryos contained a normal thoracic duct. In contrast, there were significantly ($P<0.01$) lower percentages of embryos (9.1±3.5 and 25.7±6.1%) with a normal thoracic duct in the *zlpa*$_1$-sMO$_1$- and *zlpa*$_1$-sMO$_2$-treated groups, respectively (**Fig. 6*A***). The lower inhibitory effect of *zlpa*$_1$-sMO$_2$ to block thoracic duct formation even at a higher dosage (7.5 ng/embryo) was presumably due to its lower potency in interfering with *zlpa*$_1$ splicing, as described (Fig. 3*C*).

To confirm that *zlpa*$_1$-sMO$_1$-induced defects were due to loss of *zlpa*$_1$, we coinjected *zlpa*$_1$-sMO$_1$ with an expressing vector containing the *zlpa*$_1$ coding region, which does not contain the MO-targeting site, to see whether *zlpa*$_1$-sMO$_1$-induced defects could be rescued. Ectopic expression of *zlpa*$_1$ fully or partially rescued >80% of zebrafish larvae, which might have developed morphological defects, such as edema and the lack of a swim bladder, in the presence of *zlpa*$_1$-sMO$_1$ (Fig. 4*C*). The morphology of *zlpa*$_1$-res-

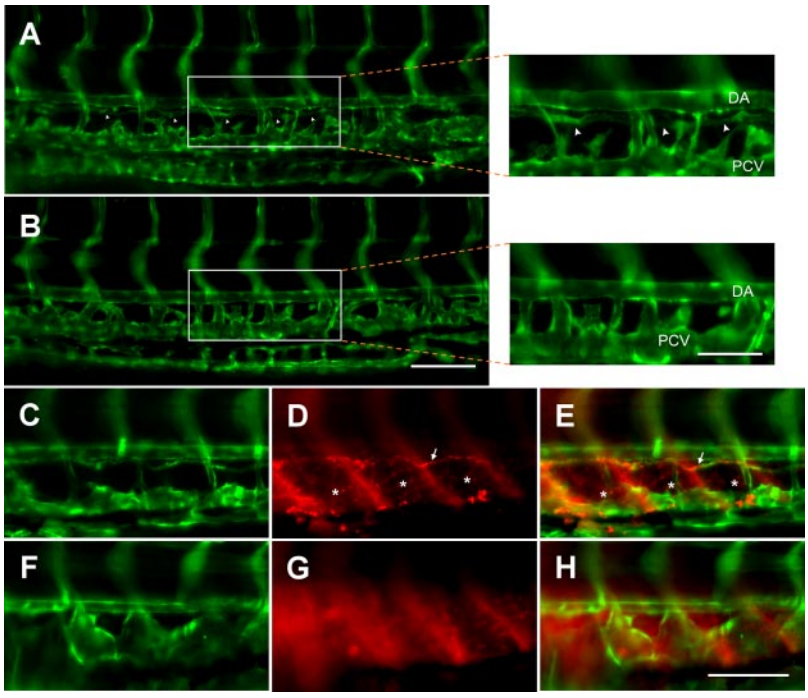

Figure 5. Knockdown of *zlpa*$_1$ inhibits formation of the thoracic duct, thus preventing lymphatic uptake. Zebrafish were aligned with the dorsal to the top and anterior to the left. Epifluorescent images collected with an ×10 objective of the lateral views of the trunk vasculature from 5-dpf *Tg(fli1:EGFP)*^{y1} zebrafish uninjected (*A*) or injected with 1.25 ng of *zlpa*$_1$ sMO$_1$ (*B*). Arrowheads indicate the thoracic duct, which is present in the control embryo (*A*), but absent from the *zlpa*$_1$ morphant (*B*). Boxed regions of *A* and *B* viewed with an ×20 objective are shown at right. Rhodamine dextran at 4.6–9.2 μg was injected intramuscularly into 5-dpf *Tg(fli1:EGFP)*^{y1} zebrafish. After overnight culture, epifluorescent images collected with an ×20 objective were photographed to reveal the vasculature (*C*, *F*) and lymphatic vessels filled with rhodamine dextran (*D*, *G*) using FITC and rhodamine filters, respectively. In addition, superimposed images of *C*, *D* and *F*, *G* are shown in panels *E* and *H*, respectively. It appears that rhodamine dextran was absorbed by the lymphatic vessels, including the thoracic duct (arrows) and blind-ended lymphatic vessels (*) between intersegmental vessels in control zebrafish (*D*, *E*), but the uptake by the thoracic duct is not apparent in the *zlpa*$_1$ morphant (*G*, *H*). DA, dorsal aorta; PCV, posterior cardinal vein. Scale bars = 100 μm (*A*, *B*); 50 μm (*A*, *B* enlargements); 100 μm (*C*–*H*).

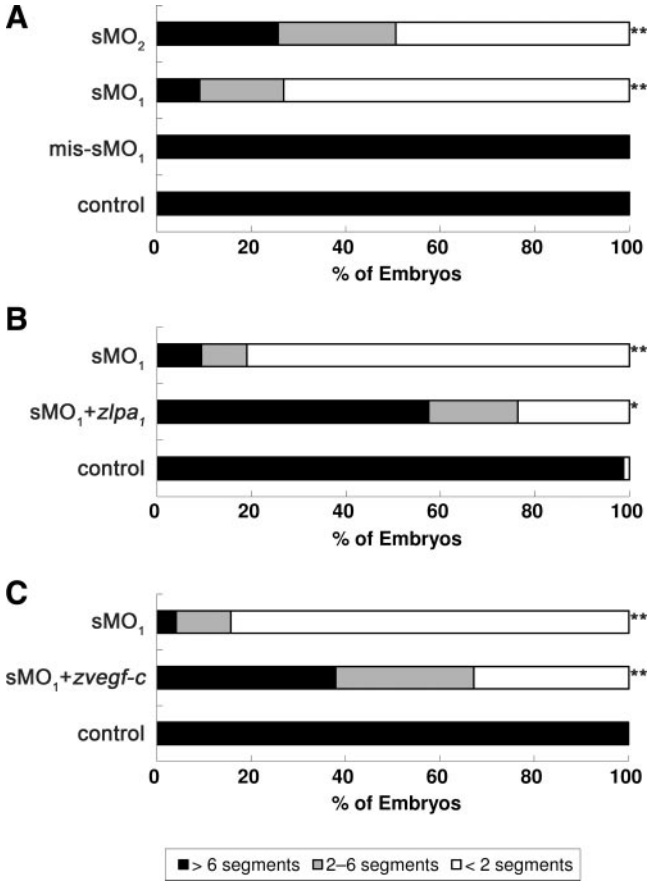

Figure 6. *zlpa$_1$* splice-blocking morpholino (sMO) inhibits thoracic duct formation and its rescue by the ectopic expression of *zlpa$_1$* or *zvegf-c*. *Tg(fli1:EGFP)^{y1}* zebrafish embryos were injected without (control) or with 1.25 ng *zlpa$_1$* sMO$_1$ (sMO$_1$) (*A*), 1.25 ng mismatched sMO$_1$ (mis-sMO$_1$), or 7.5 ng sMO$_2$ (sMO$_2$); 1.25 ng *zlpa$_1$* sMO$_1$ in the absence or presence of 100 ng of the pcDNA 3.1 vector with *zlpa$_1$* (sMO$_1$+*zlpa$_1$*) (*B*), or *vegf-c* (sMO$_1$+*zvegf-c*) at the 1-cell stage (*C*), and the length of the thoracic duct was examined at 5-dpf under an epifluorescent microscope by counting segments between 2 intersegmental vessels. Percentages of embryos with <6 segments (gray and open regions) were compared between treatments and their respective controls. *$P < 0.05$; **$P < 0.01$.

cued zebrafish larvae (*C*) was indistinguishable from that of control ones (Fig. 4*A*). The *zlpa$_1$*-rescued zebrafish larvae contained a significantly ($P<0.05$) higher percentage (57.5±12.9%) of the normal thoracic duct (see representative photograph in Supplemental Fig. S3*C*) compared to those injected with *zlpa$_1$*-sMO$_1$ only (9.4±1.0%, Fig. 6*B*). A higher percentage (18.9±4.6%) of rescued larvae was found to have a intermediately long thoracic duct (2 to 6 segments) compared to those of *zlpa$_1$* morphants (9.6±8.4%, Fig. 6*B*). Intriguingly, the lymphatic defect-inducing effect of *zlpa$_1$*-sMO$_1$ could also be partially ameliorated (37.9±3.3 and 29.3±7.0% embryos with a thoracic duct >6 segments and 2 to 6 segments, respectively; $P<0.05$) by the ectopic expression of zebrafish *vegf-c* (Fig. 6*C*, $n=4$, see representative photograph in Supplemental Fig. S3*D*).

DISCUSSION

LPA is a bioactive lipid that is thought to regulate angiogenesis in normal and tumor tissues (12, 25, 40). However, mice lacking the LPA receptors, LPA$_1$ and LPA$_1$/LPA$_2$, show no detectable defects in vasculogenesis or angiogenesis (9, 27), rendering the regulatory mechanism of LPA-mediated vascular responses a puzzle. In this study, we report that zLPA$_1$ was expressed in the dorsal aorta and vicinity, and the knockdown of zLPA$_1$ resulted in high penetrance loss of the thoracic duct. The loss of the thoracic duct was specific to a reduction in LPA$_1$ activity, since it was consistently observed even at low *zlpa$_1$* MO dosages and could be rescued by the ectopic expression of *zlpa$_1$*. In addition, overexpression of *zvegf-c*, a well-known lymphangiogenic factor, was also able to partially ameliorate the *zlpa$_1$*-morphant phenotypes. This further confirms the involvement of LPA$_1$ in mediating lymphangiogenesis in zebrafish. To our knowledge, this is a novel function of LPA receptor, and this is the first study implicating a G-protein-coupled receptor in the regulation of lymphangiogenesis.

Lysophospholipids, including LPA and sphingosine 1-phosphate (S1P), have long been implicated in cardiovascular development, where S1P appears to play a more prominent role in this aspect (41). The zebrafish mutant, *Miles apart*, which encodes S1P$_2$, was found to result in cardia bifida (42). Although this is the first instance to suggest the role of S1P receptor in vertebrate development, the S1P$_2$-null mice have no apparent anatomical or physiological defects at birth (43, 44). On the other hand, S1P$_1$-null mice exhibit strong defects in vascular smooth muscle recruitment, embryonic hemorrhage, and death (45). In contrast to the prominent roles of S1P receptor in cardiovascular development, the LPA receptor-null mice do not reveal notable defects in the cardiovascular system (9, 27). However, half of the LPA$_1$ knockout mice died between late embryonic development and weaning. Although the neonatal death of those LPA$_1$ knockout mice was attributed to a suckling defect, it would be interesting to examine the integrity of the lymphatic system of those knockout mice. In addition, autotoxin-deficient mice die at embryonic day 9.5 showing profound vascular defect in yolk sac (26). It further supports that LPA may work *via* one or more of its receptors to regulate vascular development.

There are at least five mammalian LPA receptors been identified, but only two of them, LPA$_1$ (9, 10, 27)and LPA$_3$ (28) have known *in vivo* functions by using the knockout mouse approach. More recently, a G protein-coupled receptor, P2Y5, has been shown to be a novel LPA receptor, which is involved in maintenance of human hair growth (46). To explore zebrafish LPA receptors, we searched the zebrafish genome database and found LPA$_1$, LPA$_2$ (*NP_001003578*), LPA$_3$ (*XP_694990*), and a predicted sequence of LPA$_4$ (*XP_001334713*). We have cloned LPA$_{1-3}$ but failed to obtain the LPA$_4$, which only has a predicted sequence in the database. To compare their sequence similarity

to mammalian LPA_1, those zebrafish LPA_{1-4} sequences were aligned with sequences of human and mouse LPA_1 (Supplemental Fig. S4). Sequence alignment showed that zebrafish LPA_1 is the closest homolog to mammalian LPA_1. The sequence similarities of zebrafish LPA_{1-4} compared to human or mouse LPA_1 are 89, 52, 45, and 12/13%, respectively (Supplemental Fig. S4*B*). In addition, the phylogenetic tree analysis further reveals that zebrafish LPA_1 is indeed the closest homolog of mammalian LPA_1 (Supplemental Fig. S4*C*). The $zLPA_1$ contains 7 putative transmembrane domains (Fig. 1*B*). In addition, Valentine *et al.* (47) have identified 5 critical LPA binding amino acid residues, including R3.28, Q3.29, W4.64, D5.38, and K7.36, which correspond to the $zLPA_1$ amino acid 106, 107, 168, 186, and 276 (Fig. 1*A*), respectively, in the LPA receptors. Those amino acid residues are conserved except D5.38, in which an aspartic acid is replaced by an asparagine, in $zLPA_1$ as indicated in Fig. 1*A*. With the high sequence similarity and the conservation of ligand-binding residues to mammalian LPA_1, the $zLPA_1$ is more likely to be an LPA receptor.

In this study, we confirmed the ubiquitous expression of *zlpa$_1$* in various adult tissues (Fig. *2G*) compared to its mouse homolog (8). The WISH analysis demonstrated that $zlpa_1$ expression spreads through the entire blastodisc at a low level and is then restricted to adaxial cells, head, and tail buds at somatogenesis (Fig. 2*A*, *B*). Two types of muscle precursors are reported in zebrafish somites. Adaxial cells are located next to the notochord and form future slow-muscle fibers, whereas lateral somitic cells give rise to future fast-muscle cells (48, 49). *zlpa$_1$* appears only to be expressed in nonmigratory adaxial cells, since it was still located at the site juxtaposed to the notochord at the 18-somite stage (Fig. 2*B*). This expression pattern is similar to that of *engrailed 1b* and the lymphatic master gene, *prox1*, at similar stages (50, 51). These nonmigratory adaxial cells are muscle pioneers, which are known to be future slow-muscle cells that constitute the horizontal myoseptum (48, 49). After 24 hpf, *lpa$_1$* expression was heavily condensed in the eye and brain regions (Fig. 2*C*, *D*), which is similar to that of its mammalian homologue (8). Its expression was also found in the vicinity of the dorsal aorta (Fig. 2*E*) where *vegf-c* was expressed (52) The z*lpa$_1$* expression domain encompassed only part of the dorsal aorta (Fig. 2*E*). In contrast, the *zvegf-c* expression domain enclosed the entire dorsal aorta (data not shown). These partially overlapping signals of *zlpa$_1$* and *zvegf-c* at the dorsal aorta suggest a possible linkage between them. In addition, the z*lpa$_1$* expression domain appeared to include the hypochord, a transient structure in intimate association with notochord and dorsal aorta (53). The hypochord is known to express VEGF and is essential for the development of dorsal aorta (54). The expression of $zLPA_1$ in the hypochord and dorsal aorta suggests a role of $zLPA_1$ in vasculargenesis. However, knockdown of $zLPA_1$ appeared to have limited effects on blood vessels in zebrafish. It implies that the $zLPA_1$ may not be essential or other factors may be complementary to its regulation of blood vessels.

The lack of noticeable morphological defects observed for *zlpa$_1$* morphants in the early stages suggests that $zPLA_1$ is not essential for early development, including blood vasculature formation. In contrast, the later appearance of edema in *zlpa$_1$* morphants implies a tissue fluid imbalance. The requirement of adequate fluid balance increases with growth of zebrafish larvae. Therefore, the need for a functioning thoracic duct increases later in larval development. As shown in Supplemental Fig. S2 and also in results by Yaniv *et al.* (39), a nearly complete thoracic duct is not formed until 5 dpf in zebrafish. The development of the thoracic duct coincides nicely to our observation that the edema of *zlpa$_1$* morphants was also shown gradually after 4 or 5 dpf. Our observation that a functional thoracic duct was not formed on the treatment of *zlpa$_1$*-MO (Fig. 5) further indicates that the edema was due to the lack of a thoracic duct. The blood vessels appeared normal prior to 5-dpf stage; however, we can not rule out the possibility that the vascular leakage might also contribute to the formation of edema in those *zlpa$_1$* morphants.

The late appearance of *zlpa$_1$*-MO phenotype raises the concern that it might not be a primary effect of MO since most MOs' activity are known to last for only 3 or 4 days in zebrafish embryos. In this regard, our RT-PCR analysis unequivocally showed that the *zlpa$_1$*-MO still retained its splice-blocking activity in 5-dpf embryos, the oldest embryos examined in this study (Fig. 3*D*). In addition, the splice blocking of antisense MO oligonucleotides is a commonly used approach to effectively knock down gene activity in zebrafish. However, one concern could be that the observed *zlpa$_1$*-morphant phenotypes might be due to the dominant-negative effects of aberrantly translated proteins, but not the effects of *zlpa$_1$* gene knockdown. Although MO-generated splice variants may be translated, they are often degraded after the first translation by nonsense-mediated decay, especially if the splice modification results in a frameshift. To further address this issue, we have sequenced the PCR products generated by the splice variants of sMO_1 and sMO_2. Both splice variants, as expected, had eliminated the *zlpa$_1$* Exon 2, as shown in Supplemental Fig. S1. By the presence of a translation start site (ATG), we could identify 7 potential protein products with only one inframe protein that might be synthesized (Supplemental Fig. S1). With the assumption that those frameshift products were more likely to be degraded, we only discuss the possible effect of the inframe protein further. This possible inframe product is a 59-amino acid protein that comprises the end of the 7th transmembrane domain and the rest of C-terminal tail. By blasting this 59-amino acid sequence to the zebrafish protein database, there were only 5 hits except $zLPA_1$ (data not shown). A hypothetical protein (*XP_694990.2*) was found to have a highest identity of

18 in 25 amino acids. With the low-sequence homologies to other zebrafish proteins, even if this 59-amino acid protein were to produce a dominant-negative effect, it would still be specific to the $zLPA_1$. Thus, the possible dominant-negative effect should not affect our conclusion. Furthermore, along with the *zlpa$_1$* rescue experiments and consistent phenotypes obtained by the sMO_2 (but not the 5-bp mismatched sMO_1), we conclude that the loss of thoracic duct is specifically induced by knocking down $zLPA_1$. We currently do not know whether the block of thoracic duct formation was a direct consequence of $zLPA_1$ knockdown; however, LPA has been shown to prime LPA receptor-expressing cells such as astrocytes to produce a specific secondary response to promote neuronal differentiation (55). Therefore, the loss of the thoracic duct in *zlpa$_1$* morphants is at least a specific secondary response by *zlpa$_1$* knockdown, if not a primary one.

The present study suggests a possible link of LPA_1 with lymphangiogenesis. LPA_1-mediated lymphangiogenesis may be dependent on or independent of VEGF-C signaling. Although LPA did induce LPA_1-dependent expression of *vegf-c* in HUVECs in our preliminary trials (unpublished results), we failed to demonstrate consistent modulation of *vegf-c* expression on *lpa1* knockdown or ectopic expression in zebrafish embryos by real-time PCR or WISH analyses (data not shown). These results imply that LPA and VEGF-C may work in parallel to modulate lymphatic vessel development. This finding is important because it provides a clue for examining how LPA may participate in cancer formation. LPA stimulates cell proliferation, migration, and survival. These LPA-evoked responses are hallmarks of tumor growth and metastasis (56). Thus, when significant LPA levels were found to be present in malignant effusions and its receptors were expressed in several human cancer cells, it became an emerging candidate for a cancer marker (4). LPA was also suggested to be a tumor inducer due to its capability of inducing cell motility and invasiveness, especially in both ECs (14–16) and tumor cells (57). VEGF-C and its receptor, VEGFR-3, are expressed in lymphatic endothelial cells and a variety of human tumor cells. Therefore, activation of the VEGF-C/VEGFR-3 axis in conjunction of LPA_1 signaling in lymphatic ECs can facilitate metastasis by stimulating lymphangiogenesis within and around tumors (58–60).

In summary, we have discovered a novel function of the LPA receptor, LPA_1, as being a key receptor for mediating thoracic duct formation in zebrafish. Signaling for LPA_1-mediated lymphangiogenesis possibly occurs in parallel to that of VEGF-C. These findings can assist our understanding of the molecular control of lymphangiogenesis *in vivo*, as well as help in unraveling the possible role of LPA in tumor metastasis through its regulation of lymphangiogenesis.

This work was supported by a grant (NSC95–2311-B-002–015-MY3) to S.J.L. from the National Science Council of Taiwan. FJ

REFERENCES

1. Adams, R. H., and Alitalo, K. (2007) Molecular regulation of angiogenesis and lymphangiogenesis. *Nat. Rev. Mol. Cell Biol.* **8,** 464–478
2. Oliver, G. (2004) Lymphatic vasculature development. *Nat. Rev.* **4,** 35–45
3. Cleaver, O., and Melton, D. A. (2003) Endothelial signaling during development. *Nat. Med.* **9,** 661–668
4. Mills, G. B., and Moolenaar, W. H. (2003) The emerging role of lysophosphatidic acid in cancer. *Nat. Rev. Cancer* **3,** 582–591
5. Anliker, B., and Chun, J. (2004) Cell surface receptors in lysophospholipid signaling. *Semin. Cell Dev. Biol.* **15,** 457–465
6. Meyer zu Heringdorf, D., and Jakobs, K. H. (2007) Lysophospholipid receptors: signalling, pharmacology and regulation by lysophospholipid metabolism. *Biochim. Biophys. Acta* **1768,** 923–940
7. Moolenaar, W. H. (1999) Bioactive lysophospholipids and their G protein-coupled receptors. *Exp. Cell Res.* **253,** 230–238
8. Hecht, J. H., Weiner, J. A., Post, S. R., and Chun, J. (1996) Ventricular zone gene-1 (vzg-1) encodes a lysophosphatidic acid receptor expressed in neurogenic regions of the developing cerebral cortex. *J. Cell Biol.* **135,** 1071–1083
9. Contos, J. J., Fukushima, N., Weiner, J. A., Kaushal, D., and Chun, J. (2000) Requirement for the lpA1 lysophosphatidic acid receptor gene in normal suckling behavior. *Proc. Natl. Acad. Sci. U. S. A.* **97,** 13384–13389
10. Estivill-Torrus, G., Llebrez-Zayas, P., Matas-Rico, E., Santin, L., Pedraza, C., De Diego, I., Del Arco, I., Fernandez-Llebrez, P., Chun, J., and De Fonseca, F. R. (2008) Absence of LPA1 signaling results in defective cortical development. *Cereb. Cortex* **18,** 938–950
11. Lin, C. I., Chen, C. N., Lin, P. W., Chang, K. J., Hsieh, F. J., and Lee, H. (2007) Lysophosphatidic acid regulates inflammation-related genes in human endothelial cells through LPA_1 and LPA_3. *Biochem. Biophys. Res. Commun.* **363,** 1001–1008.
12. English, D., Kovala, A. T., Welch, Z., Harvey, K. A., Siddiqui, R. A., Brindley, D. N., and Garcia, J. G. (1999) Induction of endothelial cell chemotaxis by sphingosine 1-phosphate and stabilization of endothelial monolayer barrier function by lysophosphatidic acid, potential mediators of hematopoietic angiogenesis. *J. Hematother. Stem Cell Res.* **8,** 627–634
13. Tager, A. M., Lacamera, P., Shea, B. S., Campanella, G. S., Selman, M., Zhao, Z., Polosukhin, V., Wain, J., Karimi-Shah, B. A., Kim, N. D., Hart, W. K., Pardo, A., Blackwell, T. S., Xu, Y., Chun, J., and Luster, A. D. (2008) The lysophosphatidic acid receptor LPA_1 links pulmonary fibrosis to lung injury by mediating fibroblast recruitment and vascular leak. *Nat. Med.* **14,** 45–54
14. Lee, H., Goetzl, E. J., and An, S. (2000) Lysophosphatidic acid and sphingosine 1-phosphate stimulate endothelial cell wound healing. *Am. J. Physiol. Cell Physiol.* **278,** C612–C618
15. Panetti, T. S. (2002) Differential effects of sphingosine 1-phosphate and lysophosphatidic acid on endothelial cells. *Biochim. Biophys. Acta* **1582,** 190–196
16. Langlois, S., Gingras, D., and Beliveau, R. (2004) Membrane type 1-matrix metalloproteinase (MT1-MMP) cooperates with sphingosine 1-phosphate to induce endothelial cell migration and morphogenic differentiation. *Blood* **103,** 3020–3028
17. Wu, W. T., Chen, C. N., Lin, C. I., Chen, J. H., and Lee, H. (2005) Lysophospholipids enhance matrix metalloproteinase-2 expression in human endothelial cells. *Endocrinology* **146,** 3387–3400
18. Lin, C. I., Chen, C. N., Chen, J. H., and Lee, H. (2006) Lysophospholipids increase IL-8 and MCP-1 expressions in human umbilical cord vein endothelial cells through an IL-1-dependent mechanism. *J. Cell. Biochem.* **99,** 1216–1232
19. Schulze, C., Smales, C., Rubin, L. L., and Staddon, J. M. (1997) Lysophosphatidic acid increases tight junction permeability in cultured brain endothelial cells. *J. Neurochem.* **68,** 991–1000
20. Cerutis, D. R., Nogami, M., Anderson, J. L., Churchill, J. D., Romberger, D. J., Rennard, S. I., and Toews, M. L. (1997) Lysophosphatidic acid and EGF stimulate mitogenesis in human airway smooth muscle cells. *Am. J. Physiol.* **273,** L10–L15
21. Hayashi, K., Takahashi, M., Nishida, W., Yoshida, K., Ohkawa, Y., Kitabatake, A., Aoki, J., Arai, H., and Sobue, K. (2001) Phenotypic modulation of vascular smooth muscle cells induced by unsaturated lysophosphatidic acids. *Circ. Res.* **89,** 251–258

22. Toews, M. L., Ustinova, E. E., and Schultz, H. D. (1997) Lysophosphatidic acid enhances contractility of isolated airway smooth muscle. *J. Appl. Physiol.* **83,** 1216–1222
23. Tokumura, A., Iimori, M., Nishioka, Y., Kitahara, M., Sakashita, M., and Tanaka, S. (1994) Lysophosphatidic acids induce proliferation of cultured vascular smooth muscle cells from rat aorta. *Am. J. Physiol.Cell Physiol* **267,** C204–C210
24. Tokumura, A., Yotsumoto, T., Masuda, Y., and Tanaka, S. (1995) Vasopressor effect of lysophosphatidic acid on spontaneously hypertensive rats and Wistar-Kyoto rats. *Res. Commun. Molec. Pathol. Pharmacol.* **90,** 96–102
25. Yoshida, K., Nishida, W., Hayashi, K., Ohkawa, Y., Ogawa, A., Aoki, J., Arai, H., and Sobue, K. (2003) Vascular remodeling induced by naturally occurring unsaturated lysophosphatidic acid in vivo. *Circulation* **108,** 1746–1752
26. Van Meeteren, L. A., Ruurs, P., Stortelers, C., Bouwman, P., van Rooijen, M. A., Pradere, J. P., Pettit, T. R., Wakelam, M. J., Saulnier-Blache, J. S., Mummery, C. L., Moolenaar, W. H., and Jonkers, J. (2006) Autotaxin, a secreted lysophospholipase D, is essential for blood vessel formation during development. *Mol. Cell. Biol.* **26,** 5015–5022
27. Contos, J. J., Ishii, I., Fukushima, N., Kingsbury, M. A., Ye, X., Kawamura, S., Brown, J. H., and Chun, J. (2002) Characterization of *lpa*$_2$ (*Edg4*) and *lpa*$_1$/*lpa*$_2$ (*Edg2/Edg4*) lysophosphatidic acid receptor knockout mice: signaling deficits without obvious phenotypic abnormality attributable to *lpa*$_2$. *Mol. Cell. Biol.* **22,** 6921–6929
28. Ye, X., Hama, K., Contos, J. J., Anliker, B., Inoue, A., Skinner, M. K., Suzuki, H., Amano, T., Kennedy, G., Arai, H., Aoki, J., and Chun, J. (2005) LPA$_3$-mediated lysophosphatidic acid signalling in embryo implantation and spacing. *Nature* **435,** 104–108
29. Noguchi, K., Ishii, S., and Shimizu, T. (2003) Identification of p2y9/GPR23 as a novel G protein-coupled receptor for lysophosphatidic acid, structurally distant from the Edg family. *J. Biol. Chem.* **278,** 25600–25606
30. Lee, C. W., Rivera, R., Gardell, S., Dubin, A. E., and Chun, J. (2006) GPR92 as a new G12/13- and Gq-coupled lysophosphatidic acid receptor that increases cAMP, LPA$_5$. *J. Biol. Chem.* **281,** 23589–23597
31. Weinstein, B. M. (2002) Plumbing the mysteries of vascular development using the zebrafish. *Sem. Cell Dev. Biol.* **13,** 515–522
32. Ny, A., Autiero, M., and Carmeliet, P. (2006) Zebrafish and *Xenopus* tadpoles: small animal models to study angiogenesis and lymphangiogenesis. *Exp. Cell Res.* **312,** 684–693
33. Kimmel, C. B., Ballard, W. W., Kimmel, S. R., Ullmann, B., and Schilling, T. F. (1995) Stages of embryonic development of the zebrafish. *Dev. Dyn.* **203,** 253–310
34. Thisse, C., Thisse, B., Schilling, T. F., and Postlethwait, J. H. (1993) Structure of the zebrafish snail1 gene and its expression in wild-type, spadetail and no tail mutant embryos. *Development* **119,** 1203–1215
35. Ober, E. A., Olofsson, B., Makinen, T., Jin, S. W., Shoji, W., Koh, G. Y., Alitalo, K., and Stainier, D. Y. (2004) Vegfc is required for vascular development and endoderm morphogenesis in zebrafish. *EMBO Rep.* **5,** 78–84
36. Lai, S. L., Chang, C. N., Wang, P. J., and Lee, S. J. (2005) Rho mediates cytokinesis and epiboly via ROCK in zebrafish. *Mol. Reprod. Dev.* **71,** 186–196
37. Lawson, N. D., Scheer, N., Pham, V. N., Kim, C. H., Chitnis, A. B., Campos-Ortega, J. A., and Weinstein, B. M. (2001) Notch signaling is required for arterial-venous differentiation during embryonic vascular development. *Development* **128,** 3675–3683
38. Kuchler, A. M., Gjini, E., Peterson-Maduro, J., Cancilla, B., Wolburg, H., and Schulte-Merker, S. (2006) Development of the zebrafish lymphatic system requires VEGFC signaling. *Curr. Biol.* **16,** 1244–1248
39. Yaniv, K., Isogai, S., Castranova, D., Dye, L., Hitomi, J., and Weinstein, B. M. (2006) Live imaging of lymphatic development in the zebrafish. *Nat. Med.* **12,** 711–716
40. Hu, Y. L., Tee, M. K., Goetzl, E. J., Auersperg, N., Mills, G. B., Ferrara, N., and Jaffe, R. B. (2001) Lysophosphatidic acid induction of vascular endothelial growth factor expression in human ovarian cancer cells. *J. Natl. Cancer Inst.* **93,** 762–768
41. Birgbauer, E., and Chun, J. (2006) New developments in the biological functions of lysophospholipids. *Cell. Mol. Life Sci.* **63,** 2695–2701
42. Kupperman, E., An, S., Osborne, N., Waldron, S., and Stainier, D. Y. (2000) A sphingosine-1-phosphate receptor regulates cell migration during vertebrate heart development. *Nature* **406,** 192–195
43. Ishii, I., Ye, X., Friedman, B., Kawamura, S., Contos, J. J., Kingsbury, M. A., Yang, A. H., Zhang, G., Brown, J. H., and Chun, J. (2002) Marked perinatal lethality and cellular signaling deficits in mice null for the two sphingosine 1-phosphate (S1P) receptors, S1P$_2$/LP$_{B2}$/EDG-5 and S1P$_3$/LP$_{B3}$/EDG-3. *J. Biol. Chem.* **277,** 25152–25159
44. MacLennan, A. J., Carney, P. R., Zhu, W. J., Chaves, A. H., Garcia, J., Grimes, J. R., Anderson, K. J., Roper, S. N., and Lee, N. (2001) An essential role for the H218/AGR16/Edg-5/LP$_{B2}$ sphingosine 1-phosphate receptor in neuronal excitability. *Eur. J. Neurosci.* **14,** 203–209
45. Liu, Y., Wada, R., Yamashita, T., Mi, Y., Deng, C. X., Hobson, J. P., Rosenfeldt, H. M., Nava, V. E., Chae, S. S., Lee, M. J., Liu, C. H., Hla, T., Spiegel, S., and Proia, R. L. (2000) Edg-1, the G protein-coupled receptor for sphingosine-1-phosphate, is essential for vascular maturation. *J. Clin. Invest.* **106,** 951–961
46. Pasternack, S. M., von Kugelgen, I., Aboud, K. A., Lee, Y. A., Ruschendorf, F., Voss, K., Hillmer, A. M., Molderings, G. J., Franz, T., Ramirez, A., Nurnberg, P., Nothen, M. M., and Betz, R. C. (2008) G protein-coupled receptor P2Y5 and its ligand LPA are involved in maintenance of human hair growth. *Nat. Genet.* **40,** 329–334
47. Valentine, W. J., Fells, J. I., Perygin, D. H., Mujahid, S., Yokoyama, K., Fujiwara, Y., Tsukahara, R., Van Brocklyn, J. R., Parrill, A. L., and Tigyi, G. (2008) Subtype-specific residues involved in ligand activation of the endothelial differentiation gene family lysophosphatidic acid receptors. *J. Biol. Chem.* **283,** 12175–12187
48. Devoto, S. H., Melancon, E., Eisen, J. S., and Westerfield, M. (1996) Identification of separate slow and fast muscle precursor cells in vivo, prior to somite formation. *Development* **122,** 3371–3380
49. Stickney, H. L., Barresi, M. J., and Devoto, S. H. (2000) Somite development in zebrafish. *Dev. Dyn.* **219,** 287–303
50. Thisse, B., and Thisse, C. (2004) Fast release clones: a high throughput expression analysis. Retrieved October 19, 2007, from http://zfin.org; ZFIN ID: ZDB-PUB-040907-1
51. Thisse, B., and Thisse, C. (2005) High throughput expression analysis of ZF-models consortium clones. Retrieved October 19, 2007, from http://zfin.org; ZFIN ID: ZDB-PUB-051025-1
52. Covassin, L. D., Villefranc, J. A., Kacergis, M. C., Weinstein, B. M., and Lawson, N. D. (2006) Distinct genetic interactions between multiple Vegf receptors are required for development of different blood vessel types in zebrafish. *Proc. Natl. Acad. Sci. U. S. A.* **103,** 6554–6559
53. Eriksson, J., and Lofberg, J. (2000) Development of the hypochord and dorsal aorta in the zebrafish embryo (*Danio rerio*). *J. Morphol.* **244,** 167–176
54. Cleaver, O., and Krieg, P. A. (1998) VEGF mediates angioblast migration during development of the dorsal aorta in *Xenopus*. *Development* **125,** 3905–3914
55. Spohr, T. C., Choi, J. W., Gardell, S. E., Herr, D., Rehen, S. K., Gomes, F. C., and Chun, J. (2008) LPA receptor-dependent secondary effects via astrocytes promote neuronal differentiation. *J. Biol. Chem.* **283,** 7470–7479
56. Hanahan, D., and Weinberg, R. A. (2000) The hallmarks of cancer. *Cell* **100,** 57–70
57. Imamura, F., Horai, T., Mukai, M., Shinkai, K., Sawada, M., and Akedo, H. (1993) Induction of in vitro tumor cell invasion of cellular monolayers by lysophosphatidic acid or phospholipase D. *Biochem. Biophys. Res. Commun.* **193,** 497–503
58. Akagi, K., Ikeda, Y., Miyazaki, M., Abe, T., Kinoshita, J., Maehara, Y., and Sugimachi, K. (2000) Vascular endothelial growth factor-C (VEGF-C) expression in human colorectal cancer tissues. *Brit. J. Cancer* **83,** 887–891
59. Niki, T., Iba, S., Tokunou, M., Yamada, T., Matsuno, Y., and Hirohashi, S. (2000) Expression of vascular endothelial growth factors A, B, C, and D and their relationships to lymph node status in lung adenocarcinoma. *Clin. Cancer Res.* **6,** 2431–2439
60. Su, J. L., Yen, C. J., Chen, P. S., Chuang, S. E., Hong, C. C., Kuo, I. H., Chen, H. Y., Hung, M. C., and Kuo, M. L. (2007) The role of the VEGF-C/VEGFR-3 axis in cancer progression. *Brit. J. Cancer* **96,** 541–545

Received for publication January 29, 2008.
Accepted for publication June 12, 2008.